Pressure effects on structure and dynamics of metallic glass-forming liquid

Yuan-Chao Hu,[1,2] Peng-Fei Guan,[3,a)] Qing Wang,[2,4] Yong Yang,[2,a)] Hai-Yang Bai,[1] and Wei-Hua Wang[1,a)]
[1]*Institute of Physics, Chinese Academy of Sciences, Beijing 100190, China*
[2]*Centre for Advanced Structural Materials, Department of Mechanical and Biomedical Engineering, City University of Hong Kong, Kowloon, Hong Kong, China*
[3]*Beijing Computational Science Research Center, Beijing 100094, China*
[4]*Laboratory for Microstructures, Institute of Materials Science, Shanghai University, Shanghai 200072, China*

(Received 3 November 2016; accepted 29 December 2016; published online 13 January 2017)

Although the structure and dynamics of metallic glass-forming liquids have been extensively investigated, studies of the pressure effects are rare. In the present study, the structural and dynamical properties of a ternary metallic liquid are systematically studied via extensive molecular dynamics simulations. Our results clearly show that, like isobaric cooling, isothermal compression could also slow down the dynamics of metallic liquid, leading to glass formation. However, the temperature- and pressure-induced glass transitions differ in the formation of local coordination structures and the variation of fragility. The increase of the kinetic fragility with increasing pressure is also accompanied by a monotonic structural fragility change. These findings may suggest a link between dynamics and structure. In addition, with increasing pressure, the dynamics becomes more heterogeneous, as revealed by the non-Gaussian parameter and dynamic correlation length. Here the length scales of both slow and fast domains are examined and discussed by analyzing the four-point dynamic structure factor associated with spatial correlations of atomic mobility. These correlation lengths coexist in the metallic liquids and grow comparatively in the considered temperature and pressure ranges. Finally, the scaling relation between the relaxation times and correlation lengths is discussed, which is found to be consistent with the spirit of Adam-Gibbs and random first-order transition theories. *Published by AIP Publishing.* [http://dx.doi.org/10.1063/1.4973919]

I. INTRODUCTION

As a new member to the glass family, metallic glasses (MGs) attracted tremendous interests over the past few decades because of their scientific importance and technological relevance.[1–4] In the absence of any long-range crystalline order, MGs exhibit unusual properties, such as high specific strength,[5] ultrahigh fracture toughness,[6] superior thermoplastic formability,[7,8] good biocompatibility,[9,10] and high activity in electrocatalysis,[11] which make them a promising candidate material for a wide range of applications. On the other hand, due to the relatively simple atomic structures compared to the polymeric and silicate glassy systems, MGs are usually considered as ideal model systems to study the role of many-body interactions in the mythological phenomena of the glass transition.[12]

Conventionally, MGs are obtained by cooling metallic liquids from above the melting point down to below the glass transition temperature, T_g, at a sufficiently high cooling rate to avoid crystallization. When approaching T_g, the thermal energy for atomic rearrangement plummets rapidly, which results in a kinetically frozen non-equilibrium configuration trapped in a potential well on the potential energy landscape. Consequently, the structural relaxation time increases dramatically leading to glass formation when it exceeds the experimental observation time. During glass transition, one most prominent but intriguing phenomenon is the nearly invariant structure detected by X-ray diffraction and neutron scattering, although liquid dynamics slows down by more than ten orders of magnitude.[13] In light of this interesting behavior, finding a structural "signature" for the glass transition has been a matter of intensive research in condensed matter physics and material sciences. In previous works, some methods like bond-orientational order[14,15] and Voronoi tessellation[16] were exploited to characterize the structure of disordered states. The latter is more frequently utilized in MGs and is also employed in this study to characterize the hidden structural evolution in the supercooled metallic liquids.

Other than temperature, hydrostatic pressure is another variable that could be used to tune the properties of materials.[17–21] Like conventional ultrafast quenching, isothermal compression could also trigger glass transition according to the jamming phase diagram.[22] Although some high pressure properties of MGs have been investigated previously,[20,23–25] there were few studies focusing on pressure effects on the structure and dynamics of metallic liquids. As of today, the effects of pressure on the atomic structure and dynamical behaviors of supercooled melts, such as fragility and dynamic heterogeneities, are still unclear.

[a)]Authors to whom correspondence should be addressed. Electronic addresses: pguan@csrc.ac.cn; yonyang@cityu.edu.hk; and whw@iphy.ac.cn

As an intrinsic property to glass-forming liquids, the kinetic fragility, which characterizes how rapidly the relaxation times grow with decreasing temperature, has attracted much attention to understand the dynamic behaviors of glass-forming liquids. Thus the influence of pressure on it is of great importance.[18,26] For many normal liquids without strongly hydrogen bonds, Roland *et al.* found that the isobaric fragility always decreases with increasing pressure, but the pressure range considered was limited.[18,27] Different results were also reported even for the same glass-former glycerol since it has hydrogen bonding and the structure changes with pressure. For instance, some studies[28,29] reported a continuous increase in the fragility with pressure, which is different from the trend shown in Ref. 30. Moreover, recent computer simulations showed that pressure makes a model liquid more fragile.[31] In general, the issue of pressure effects on fragility is controversial, and particularly, the pressure effects in metallic glass-forming liquids have not yet been well explored. Since isobaric cooling and isothermal compressing are two possible routes to fabricate MGs, the question of whether the effects of temperature and pressure on fragility are similar or not is still open to date.

When temperature is reduced, the atoms/molecules move collectively and the dynamics of glass-forming liquids becomes inhomogeneous, manifesting the existence of large difference in the atomic/molecular mobility in different domains. These distinct areas could be termed as "slow" and "fast" regions of which the size and lifetime increase with decreasing temperature. Consequently, the activation energy required for these cooperative rearrangements grows rapidly when the temperature approaches T_g. This heterogeneous feature demonstrates the presence of growing length scales that characterize the spatial extent of cooperatively rearranging regions or the spatial heterogeneities of local dynamics.[32–36] One of the most frequently studied length scales is the dynamic correlation length ξ_4 extracted from a dynamic, time-dependent, four-point structure factor $S_4(q,t)$ that associates with the spatial correlation of atomic mobility.[37] Compared to the regular two-point correlation functions, the high order correlation function is more powerful in capturing the dynamic properties of glass-forming liquids. To calculate $S_4(q,t)$, an overlap function $Q(t)$ (defined below) is defined to characterize atomic mobility over a time interval t. The corresponding dynamic susceptibility $\chi_4(t)$ that measures the total fluctuations of the two-point correlation function $Q(t)$ denotes the correlation volume of local dynamics. In previous works, only the spatial correlation length of immobile atoms or slow domains was studied.[33] However, the study of the dynamic correlation length in metallic glass-forming liquids is rare, compared to model liquids and colloidal suspensions. Moreover, according to the heterogeneous viewpoint of supercooled liquids, there should also be some fast regions and the size should also increase first during cooling. Although atomic mobility decreases when temperature drops, the dynamics would be more localized, not only for "slow" atoms but also for "fast" ones (as discussed below). Therefore, the correlation lengths of both fast and slow domains are worth studying.

To understand the glass transition, it is theoretically appealing to have a relationship between structural relaxation time τ_α and correlation length ξ, which, however, remains as an ongoing research topic for various glass-forming liquids.[33,38,39] The mode-coupling theory predicts a power-law description, $\tau_\alpha \sim \xi^z$, while Adam and Gibbs proposed an exponential form to describe the relation between time scale and length scale, $\tau_\alpha \sim \exp\left(\xi^\vartheta\right)$, where $\vartheta = 3$.[35] In the framework of Random First-Order Transition (RFOT) theory, a similar relationship to the Adam-Gibbs theory was proposed but with ϑ remaining a parameter.[36] Interestingly, these scaling relations seemingly exclude any influences from chemical compositions and thermodynamic conditions. This suggests that, when the relaxation times are plotted as a function of the length scale, all data should collapse on a master curve. However, it remains unknown currently whether there are some length scales of dynamic heterogeneities in metallic glass-forming liquids. If there is, what is the possible relationship between the length scales and the relaxation times.

To address the aforementioned important issues, we carried out extensive computer simulations to study the structure and dynamics of a ternary metallic glass-forming liquid subjected to high pressures. Although both isothermal compressing and isobaric cooling induce glass formation, the resultant static structure and dynamical properties are different. By analyzing the four-point dynamic structure factor, the dynamic correlation lengths of the slow and fast regions were calculated. We found that the relationship between the relaxation times and the correlation lengths for the whole range of the data could be well captured by the scaling law within the spirit of Adam-Gibbs theory and RFOT theory.

II. SIMULATION DETAILS

Molecular dynamics simulations were performed by utilizing the open source code-LAMMPS.[40] The interatomic interactions of $Zr_{50}Cu_{44}Al_6$ metallic glass-forming liquids were described by the optimized embedded atom method (EAM) potential provided by Sheng *et al.*[41] Briefly, the interatomic potential was obtained through the fitting of the potential energy surfaces of the Zr–Cu–Al system. The potential energy of an embedded atom i is given by $E_i = F_\alpha\left(\sum_{j\neq i}\rho_\beta\left(r_{ij}\right)\right) + \frac{1}{2}\sum_{j\neq i}\varphi_{\alpha\beta}\left(r_{ij}\right)$, where F is the embedding energy which is a function of the atomic electron density ρ, φ is a pair potential interaction, and α and β are respectively the element types of atoms i and j. The multi-body nature of the EAM potential is a result of the embedding energy term.[41] Initially, 10 000 atoms of the designed composition were generated in a cubic box randomly, with periodic boundary conditions applied in three directions. After equilibrating at 2000 K by holding different external hydrostatic pressures P (P = 0, 1.0, 2.0, 4.0, 8.0, 10.0, 12.0, 14.0, 18.0 GPa) under the isobaric-isothermal (NPT) ensemble for at least 1.0 ns, samples were quenched to 300 K at a rate of 1.0 K ps^{-1}. During these processes, configurations at temperatures of interest were collected. At each temperature, the samples were allowed to relax to equilibrium under NPT ensemble. Then the ensemble

was switched to the canonical ensemble (NVT) for production runs after equilibration. The combination of NPT and NVT simulations was intended to mimic the high pressure experimental conditions. For all simulations, the time step to integrate the equation of motion was 2 fs. The temperature and pressure were maintained by the *Nosé-Hoover* thermostat and barostat.

III. RESULTS AND DISCUSSION

A. Static structure characterizations

One of the most prominent phenomenological characteristics of the glass transition is that the dramatic slowdown of dynamics is not accompanied by any apparent structure change, as characterized by any two-point density-density correlation functions. However, previous studies already showed that there are some locally preferred structures that could affect or dominate glassy dynamics. But they can only be characterized from either high order structural analyses or geometrical descriptions.[13,42,43] Theoretically, the application of high pressure could squeeze out "free volume," leading to denser packing of local structures. However, apart from this trivial effect of densification, it is elusive how pressure influences the structure and dynamics of supercooled metallic liquids. In this subsection, we study the static structure of the metallic glass-forming liquid under different temperatures and pressures. The structure is characterized by pair correlation functions g(r), structural entropy S_2, and the averaged five-fold local symmetry parameter W.[42,44] The structure evolutions could be quantified through these parameters when temperature or pressure is changed.

The static structure of the metallic liquids at different temperatures and pressures was first studied by the two-point pair correlation function g(r). For isotropic systems, g(r) is defined as

$$\mathrm{g}(r) = \frac{1}{N\rho}\sum_{i=1}^{N}\sum_{j\neq i}^{N}\left\langle \delta\left(\mathbf{r}+\mathbf{r}_j-\mathbf{r}_i\right)\right\rangle, \tag{1}$$

where N is the atom number, ρ is the overall number density, and $\mathbf{r}_i$ is the position vector of atom i. The bracket means thermal average over the configurations in equilibration. g(r) represents the probability of finding two atoms separated by a position vector $\mathbf{r}$. Figures 1(a) and 1(b) show the represented results of overall g(r) at 4.0 GPa and 1200 K, respectively. The disappearance of sharp peaks in g(r) evidences the absence of crystallites in the metallic liquids. The overall effects of temperature and pressure on the static structure are quite similar. After isobaric cooling and isothermal compressing, the samples are densified to different degrees. The presence of the medium-range order is observed from the broadening and splitting of the second peak, while for the first coordination shell, the short-range order becomes stronger and denser for the two routines.[45,46] The evolution of the normalized peak amplitudes $g_{r,\max}$ of the first, second, and third peaks are shown in Figs. 1(c) and 1(d) with reducing temperature and increasing pressure, respectively. The increase of $g_{r,\max}$ for all these peaks suggests that both compression and cooling make the system ordered, but with different sensitivities. Compared to the improved medium-range order indicated by the second and third coordination shells, the enhancement of the short-range order is much more remarkable. Moreover, at higher temperatures (Fig. 1(c)) and lower pressures (Fig. 1(d)), or equivalently in the "shallow" supercooled states, the increase of $g_{r,\max}$ is linear. However, the densification of the first and second shells slows down when the liquid is more deeply supercooled, especially for the short-range order. Similar findings were observed at other temperatures and pressures. In principle, this behavior could be related to the compressibility of the system.

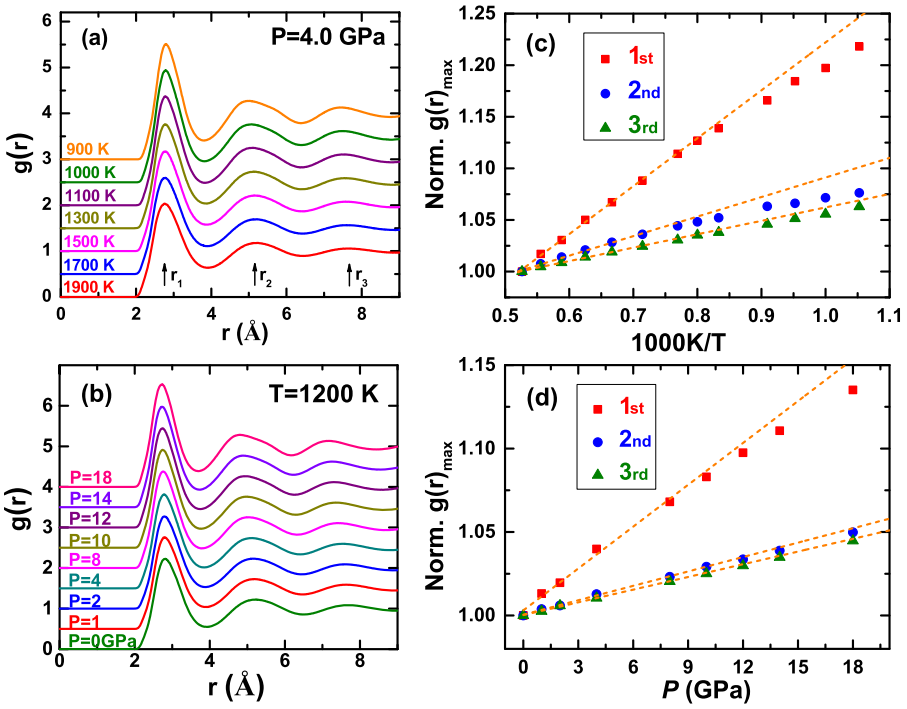

FIG. 1. Pair correlation functions of the metallic liquids during isobaric cooling (P = 4.0 GPa, (a)) and isothermal compressing (T = 1200 K, (b)). The corresponding normalized peak heights of the first, second, and third peak are shown in (c) (P = 4.0 GPa) and (d) (T = 1200 K). In the cooling and compressing processes, the structure is densified to different degrees for different peaks. The dashed lines in (c) and (d) are linear fittings to the high temperature or low pressure data.

To examine the differences of local structures in more detail for the multicomponent metallic liquids, we studied the evolution of the partial pair correlation functions $g_{\alpha\beta}(r)$ (e.g., Zr–Cu and Cu–Cu) at 4.0 GPa and 1200 K and extracted the corresponding first peak values $g_{\alpha\beta}(r)_{max}$. Figure 2 shows the normalized magnitudes of the first peak of different atomic pairs. Note that the Al–Al pair is not included due to its low concentration. Evidently, all atomic pairs become more densely packed when the temperature is decreased or the pressure is increased. However, their sensitivities to temperature and pressure are different. According to the normalized first peak amplitude, both pressure and temperature have an effect on promoting the coordination of Cu with Al remarkably; however, such an effect is moderate for Zr–Cu and Zr–Al pairs. The Zr–Zr pair is almost insensitive to pressure, but its quantity rises up when temperature decreases. In contrast, the formation of Cu–Cu pair is promoted remarkably during isothermal compression but only grows weakly in the isobaric cooling process. These findings indicate that, although both decreasing temperature and increasing pressure could densify the overall structure of the metallic liquid to some degrees, their influences on the local coordination structures are distinct. High pressure facilitates the coordination of Cu with Al and Cu, which leads to more locally ordered structures around Cu, like full icosahedra, due to the comparative radii of Cu and Al (r_{Cu}/r_{Al} = 1.27 Å/1.43 Å ≅ 0.888).[45,47] Nevertheless, temperature shows a weaker influence on Cu coordination but a much stronger effect on Zr. The different roles of pressure and temperature in modifying the local structures may result in different dynamical behaviors.

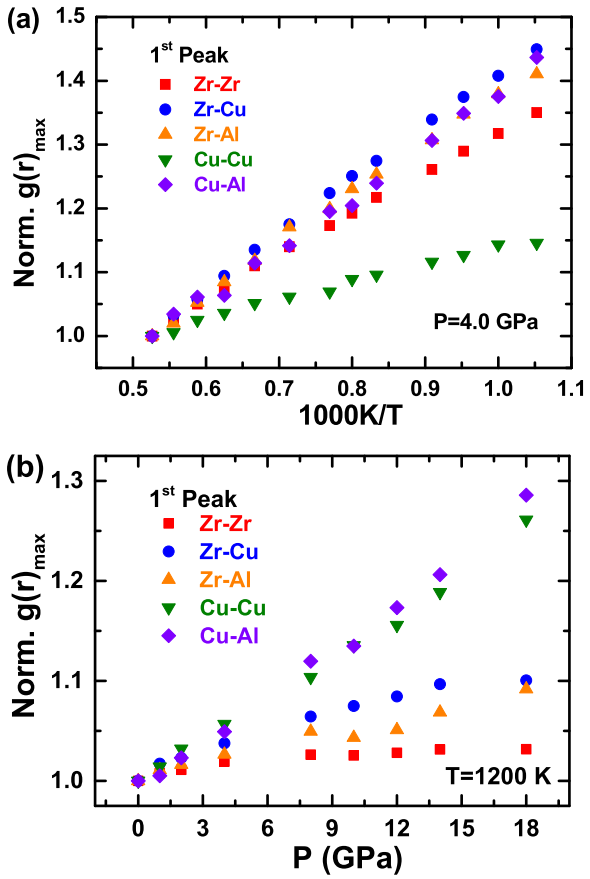

FIG. 2. The normalized first peak heights of partial pair correlation functions for different pairs during cooling (P = 4.0 GPa) and compressing (T = 1200 K). It is obvious that the effects of temperature and pressure on local coordination structures are different.

According to the Adam-Gibbs theory,[35] entropy plays important roles in the glass transition and the drastic increase of shear viscosity is ascribed to the decrease of configurational entropy, i.e., reduction in the number of available minima on the multidimensional potential energy landscape. At the ideal glass transition point, configurational entropy vanishes, and consequently, the viscosity or relaxation time is speculated to diverge. However, determining the configurational entropy accurately is not an easy task from experiments and computer simulations. Here, to obtain an approximation to the configurational entropy, the excess entropy is utilized, which quantifies the difference between liquid and crystal entropies and decreases on approaching T_g. Theoretically, the excess entropy could be expressed as a sum of integrals over the N-body inter-atomic/molecular correlation functions that quantify both translational and orientational correlations.[48] For our atomic glass-forming system, translational correlation should be primarily important. Banerjee *et al.* also found the translational correlation accounts for 80%–90% of the excess entropy in the Lennard-Jones and the Weeks-Chandler-Andersen versions of the Kob-Andersen binary mixtures.[49] Therefore, we analyze the two-body translational correlation contribution to the excess entropy, S_2, or the "pair structural entropy,"[48] to characterize the static structure of the metallic liquids,

$$S_2 = -\frac{k_B\rho}{2}\int d\mathbf{r}\left[g(\mathbf{r})\ln g(\mathbf{r}) - (g(\mathbf{r})-1)\right], \qquad (2)$$

where k_B is the Boltzmann constant. S_2 measures the degree of ordering or confusion in the system. The lower value of S_2 indicates a more ordering state. During cooling, the formation of locally preferred structure can be associated with losing entropy, such as the medium-range crystalline order in polydisperse colloidal systems and the icosahedra in CuZr-based metallic glasses.[15] A significant advantage of using S_2 is that this quantity is experimentally measurable from the pair correlation functions obtained from synchrotron irradiation or neutron scattering. As shown in Fig. 3, S_2 decreases apparently during cooling, which is more evident under high hydrostatic pressures. When we look at a constant temperature, the value S_2 is much lower at high pressures, especially in the deeper supercooled state. These results not only indicate the formation of locally preferred structures with improved ordering during cooling but also demonstrate a more ordered state at high pressures, consistent with the previous results obtained from the pair correlation analyses.

Geometrically, Voronoi tessellation was used to characterize the local atomic structure in liquids. Based on the previous study,[42] we define the average degree of κ-fold local symmetry as $\sum_i \left(f_i^\kappa \times P_i\right)$ since $\sum_i P_i = 1.0$. P_i is the fraction of polyhedron type i. f_i^κ represents the fraction of κ-edged polygon in Voronoi polyhedron type i and is defined as $f_i^\kappa = n_i^\kappa / \sum_{\kappa=3,4,5,6} n_i^\kappa$, where n_i^κ denotes the number of κ-edged polygon in Voronoi polyhedron type i. Therefore, the average degree of five-fold local symmetry, W, can be defined

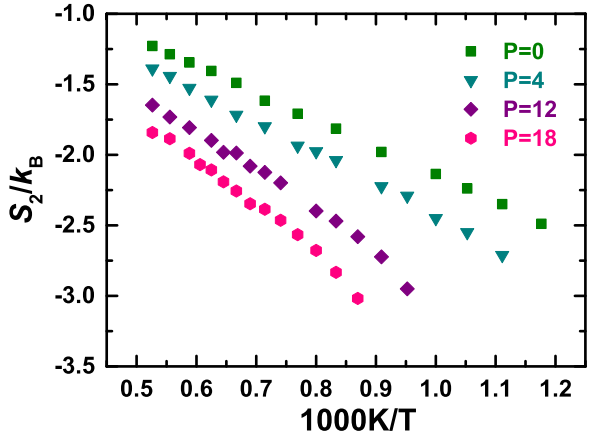

FIG. 3. The evolution of the pair structural entropy S_2 during cooling under different pressures. The lower value of the structural entropy demonstrates a more ordered local structure; thus, local ordering is improved at high pressures.

as $W = \sum_i \left(f_i^5 \times P_i\right)$. This structural parameter measures the degree of local ordering in the system. It was also found that W is capable of characterizing the structural evolution during quenching in several metallic glass-forming liquids.[42,50] The calculated W as a function of temperature is shown in Fig. 4. Obviously, W increases during cooling, which is more pronounced under high pressures. The enhanced five-fold symmetry results from squeezing out the free volume and favoring local coordination of Cu with Al/Cu induced by high pressure, which promotes the birth and growth of the locally preferred structure with preferred five-fold symmetry, such as icosahedra.[45] The formation of more ordered local structures would decrease the structural entropy S_2, especially for high pressures. This is consistent with the observations in Fig. 3.

B. Average dynamics

The advantage of MD simulations is that the trajectories of particles can be monitored accurately all the time. This allows us to study the single particle dynamics through mean-square displacement (MSD), which quantifies the travel distance of a particle over a specified time interval. The averaged MSD $\left\langle \Delta r^2(t) \right\rangle$ of an N-particle system is defined as

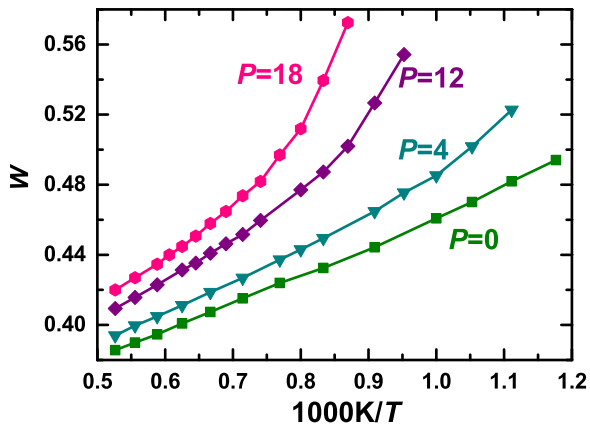

FIG. 4. The structural evolution characterized by the average five-fold local symmetry W during glass transition under different pressures. It is clear that pressure promotes the formation of denser local structures with improved five-fold local symmetry.

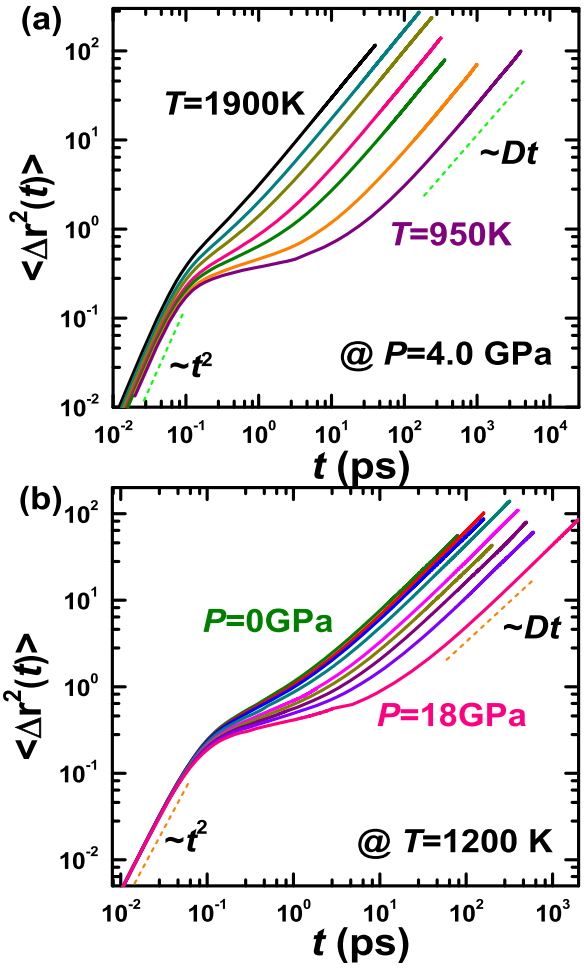

FIG. 5. The mean-square displacements during cooling ((a), P = 4.0 GPa) and compressing ((b), T = 1200 K). The temperature range in (a) is 1900, 1600, 1400, 1200, 1100, 1000, and 950 K. The pressure range in (b) is 0, 1.0, 2.0, 4.0, 8.0, 10.0, 12.0, 14.0, and 18.0 GPa. There are three regimes in the mean-square displacements, i.e., ballistic, localized, and diffusive regimes.

$\langle \Delta r^2(t) \rangle = \frac{1}{N} \langle \sum_{i=1}^{N} [\mathbf{r}_i(t) - \mathbf{r}_i(0)]^2 \rangle$. Figure 5 shows the representative MSD curves in isobaric quenching (P = 4.0 GPa) and isothermal compressing (T = 1200 K), respectively. Apparently, the dynamics slows down rapidly on cooling and compressing with the presence of long-lived plateau. When temperature decreases or pressure increases, atomic motion becomes progressively slow with $\langle \Delta r^2(t) \rangle$ exhibiting three different regimes, corresponding to the ballistic, localized, and diffusive regimes. At a very short time scale, the distance of an atom travel is linear to the elapsed time, so $\langle \Delta r^2(t) \rangle$ is proportional to t^2, as depicted in Fig. 5. The particle motion in this time scale is regarded as the ballistic movement and is not affected by its neighbors. The average velocity of particles is controlled by the thermal energy, so the $\langle \Delta r^2(t) \rangle$ curvature shifts to lower value when temperature decreases. The collapse of the data at different pressures for a constant temperature suggests that pressure affects little on this ballistic motion even the first shell packing becomes denser as pressure increases. When time grows, there is an increasingly pronounced plateau upon cooling and compressing, indicating the cage effect.[38,51] The pronounced plateau indicates that the configurational or topological excitation becomes difficult, due to the decrease

of thermal energy as temperature decreases or the increase of activation energy caused by denser packing of local structures as pressure increases. At longer times, atoms escape from the cage and undergo random walk. In this regime, MSD becomes linearly proportional to t (Fig. 5). The diffusion coefficient could be obtained in this regime.

The dramatic slowdown during the glass transition is also quantified by the spatial Fourier transformation of the van Hove correlation function, i.e., the self-intermediate scattering function $F_s(q,t)$. It characterizes the time decay of the two point density-density correlation, defined as

$$F_s(q,t) = \frac{1}{N}\left\langle \sum_{i=1}^{N} \exp\{[i\mathbf{q}\cdot[\mathbf{r}_i(t) - \mathbf{r}_i(0)]]\}\right\rangle, \quad (3)$$

where $|\mathbf{q}|$ is the wave number and is commonly taken close to the first peak position of the static structure factor.[52] Below a certain temperature, $F_s(q,t)$ shows two step relaxation behaviors, as shown in Fig. 6(a). Similar phenomena are also observed in isothermal compressing (Fig. 6(b)). As depicted in Fig. 6, while temperature defers the short time ballistic behavior, pressure has almost no influence on this motion, consistent with the results based on the averaged MSD (Fig. 5). This is because isothermal compressing just densifies the first shell packing without changing the thermal energy for short time atomic motion.

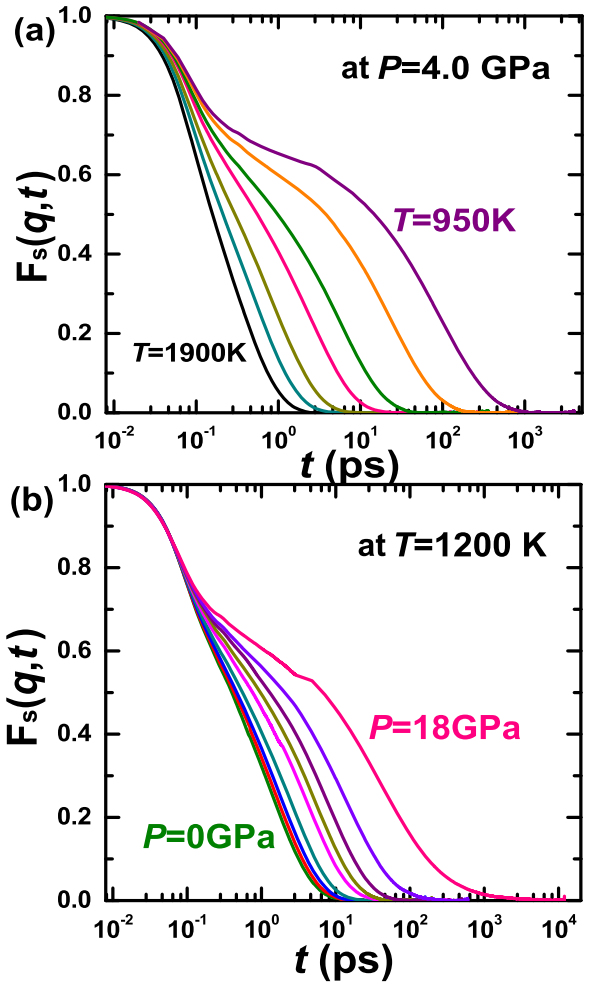

FIG. 6. The self-intermediate scattering functions during cooling ((a), P = 4.0 GPa) and compressing ((b), T = 1200 K). The temperature range in (a) is 1900, 1600, 1400, 1200, 1100, 1000, and 950 K. The pressure range in (b) is 0, 1.0, 2.0, 4.0, 8.0, 10.0, 12.0, 14.0, and 18.0 GPa.

Obviously, atomic motion becomes increasingly slow as temperature decreases or pressure increases, with $F_s(q,t)$ showing three distinct time regimes, corresponding to the ballistic, localized, and diffusive regimes in agreement with the MSD behaviors. According to the calculated $F_s(q,t)$, we can extract the structural relaxation time τ_α of the system at different temperatures and pressures. The structural relaxation time τ_α is defined as the time scale at which $F_s(q,t)$ decays to $1/e$ of its initial value $F_s(q,0)$. Figure 7(a) shows τ_α as a two-dimensional function of temperature and pressure. From the dynamic phase diagram of Fig. 7(a), both temperature and pressure could slow down the average dynamics and thus trigger metallic glass formation. Pressurized quenching could be an alternative tool to fabricate MGs. In glass-forming liquids, T_g is usually defined as the structural relaxation time or viscosity reaches a typical value.[53] In this study, we also use this empirical principle and define T_g as $\tau_\alpha(T_g) = 10^4$ ps. This well-defined kinetic T_g is approximately consistent with the values obtained from the atomic volume V-T curves in the quenching processes (not shown here), in line with the previous study.[54] Despite that the influence of pressure on dynamics is diverse in liquids, the pressure sensitivity can be reflected by the variation of T_g against pressure, as illustrated in Fig. 7(b). In comparison to other glass-forming liquids and polymers, the variation of T_g of MGs with respect to pressure is much weaker.[18,55,56] However, the similarity lies in that at low pressures, T_g increases linearly to the ascending pressure but dT_g/dP decreases with further growing pressure. This behavior is usually described by the empirical Andersson-Andersson relation,[57] $T_g(P) = k_1\left(1 + \frac{k_2}{k_3}P\right)^{1/k_2}$, where k_1, k_2, and k_3 are fitting parameters. As shown in Fig. 7(b), the correlation between T_g and P of our system could be well fitted by this empirical relation with $k_1 = 787 \pm 2$K, $k_2 = 1.5 \pm 0.2$, and $k_3 = 40 \pm 1.5$ GPa.

C. Fragility

To show how significantly the structural relaxation time τ_α of a glass-forming liquid increases towards T_g, the concept of kinetic fragility or steepness index m_T at the ambient pressure was proposed[58,59] as

$$m_T = \frac{d\log(X)}{d\left(T_g/T\right)}\Big|_{T=T_g}, \quad (4)$$

where X can be the structural relaxation time τ_α or viscosity η. Fragility represents the activation energy of glass transition and reflects the extent to which liquid dynamics deviate from the Arrhenius behavior. Some liquids, termed as strong liquids, follow the Arrhenius law and the activation energy keeps almost constant during glass transition. But in fragile liquids, the structural relaxation time increases in a highly super-Arrhenius fashion, where the activation energy increases abruptly with reducing temperature. Thus, strong liquids like silica have a lower value of m_T while fragile liquids like *o*-terphenyl have a much higher one.[26,53,58] More

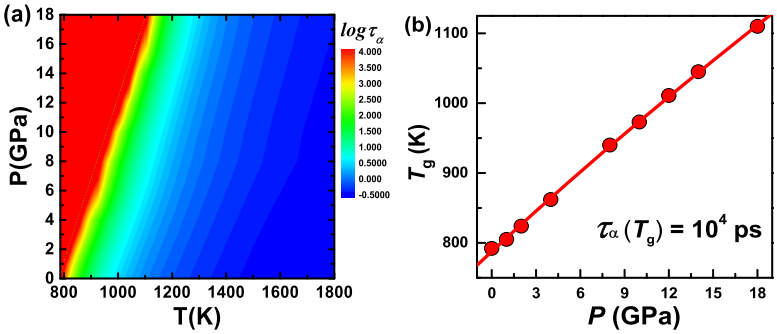

FIG. 7. (a) Two-dimensional contour plot of relaxation times as functions of temperature T and pressure P. Both isobaric cooling and isothermal compressing slow down the dynamics and induce glass transition; (b) the pressure dependence of T_g fitted to the empirical Andersson-Andersson relation with $k_1 = 787\pm2$ K, $k_2 = 1.5\pm0.2$, and $k_3 = 40\pm1.5$ GPa. T_g is defined as $\tau_\alpha\left(T_g\right) = 10$ ns.

importantly, fragility has been treated as an intrinsic property of glasses, since it correlates with many other properties. Among them, the most interesting may be the structural signature of fragility, which might indicate a structural basis for the glass transition.[60–62] However, the static structure signal from the two-point structure factor is comparatively weak, and the correlation suggested before is derived from different systems comprising various elements. Therefore, it is debatable whether there is a clear relationship between structure and fragility. Here, we investigated the relaxation time as a function of temperature T, pressure P, and the average five-fold local symmetry W, respectively. It may help us comprehensively understand the dynamic behaviors of metallic glass-forming liquids.

In the supercooled liquids, the Arrhenius relation fails to describe the glassy dynamic behaviors in the whole temperature range for many glass-forming systems. However, the relaxation times could be well described by the empirical Vogel-Fulcher-Tamman (VFT) equation,

$$\tau_\alpha = \tau_0 \exp\left(\frac{D_T T_0}{T - T_0}\right), \tag{5}$$

where τ_0, D_T, and T_0 are fitting parameters. τ_0 is the high temperature limit structural relaxation time. T_0 is the dynamical ideal glass transition temperature at which τ_α diverges hypothetically. By fitting τ_α to Eq. (5), the isobaric fragility m_T can be calculated[59] as $m_T = \frac{D_T T_0 T_g}{\ln 10 \cdot (T_g - T_0)^2}$. According to the conventional Angell plot shown in Fig. 8(a), the change of m_T is weak at low pressures. But it is evident that the temperature dependence of τ_α deviates from the Arrhenius fashion more severely when pressure is further elevated. The calculated isobaric fragility m_T is shown in the inset of Fig. 8(a). There is a remarkable increase in m_T with increasing pressure, consistent with the previous results.[29,31,63] However, this finding is different from many polymers,[18,27] indicating that pressure dependence of fragility may be material dependent. Another possible reason stems from the pressure range considered.

To parameterize the isothermal data, we employ the pressure counterpart of the VFT equation (Eq. (5)), VFT-Pressure (VFTP) relation, to fit the data, as displayed in Fig. 8(b),[64]

$$\tau_\alpha = \tau_0 \exp\left(\frac{D_P P_0}{P_0 - P}\right), \tag{6}$$

where D_P and P_0 means analogously to D_T and T_0. The glass transition pressure P_g is obtained by extrapolating τ_α to 10^4 ps. Therefore, the fragility concept is extended to the pressure variable. The isothermal fragility m_P or the steepness index with respect to pressure can be computed in analogous to m_T,

$$m_P = \frac{d\log(\tau_\alpha)}{d\left(P_g/P\right)}\Big|_{P=P_g} = \frac{D_P P_0 P_g}{\ln 10 \cdot \left(P_0 - P_g\right)^2}. \tag{7}$$

The inset in Fig. 8(b) shows an overt increase in m_P when temperature is increased, but it tends to saturate at high temperatures. Along densification by isobaric cooling or isothermal compressing, the fragility changes differently. There is an obvious increase in the isobaric fragility in the cooling process when high pressure is applied; however, isothermal fragility tends to decrease when temperature is decreased in the compressing process. From the static structure analyses, in these two processes, the variation of the local structures is different. Since the application of pressure does not change

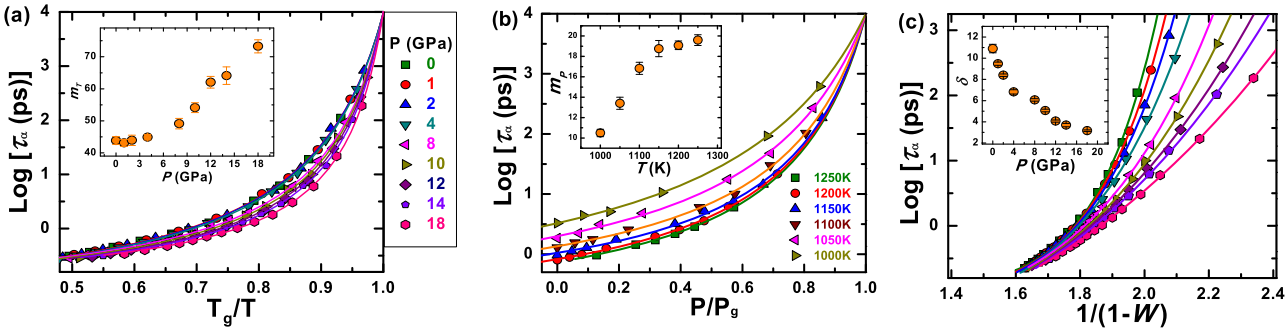

FIG. 8. (a) The Angell plot of relaxation times τ_α against T_g/T during cooling under different pressures. The solid lines are the VFT fittings (Eq. (5)). The inset is the calculated isobaric fragility. (b) The relaxation times τ_α against P/P_g during compressing at different temperatures. The solid lines are the VFTP fittings (Eq. (6)). The inset is the calculated isothermal fragility. (c) Relation between the structure parameter W and τ_α with excellent fittings to Eq. (8) under various pressures. The monotonic variation of the structural fragility is shown in the inset.

the interatomic interaction between atoms, it could be speculated that fragility may relate to the local atomic packing or locally preferred structure.[65] This connection deserves future investigation.

Establishing a fundamental structural basis for dynamics, i.e., the kinetic fragility, is of profound significance for our understanding of liquid dynamics. Here, based on Voronoi tessellation,[16] we studied the structural evolution during cooling under different external pressures. In the previous study,[42] we found that the structure parameter, W, well describes the structure in metallic glass transition and established the straightforward relationship between structure and dynamics through

$$\tau_\alpha = \tau_0 \exp \frac{A}{(1-W)^\delta}, \tag{8}$$

where A and δ are fitting parameters. More details about Eq. (8) can be found in Ref. 42. We should mention that δ reflects the sensitivity of τ_α to the structural variation similar to the meaning of isobaric fragility m_T. Thereby it is treated as the structural fragility. As pressure induces densification, the five-fold symmetry is enhanced at high pressures (Fig. 4). Larger W results in more severe frustration and impedes crystallization because of the incompatibility between five-fold symmetry and crystallographic symmetry. Thus glass transition is promoted, as discussed before. Recently, Taffs and Patrick Royall[66] tuned the degree of five-fold symmetry in a model hard sphere system and probed its role in suppressing crystallization. They found that the nucleation rate is strongly suppressed when five-fold symmetry is increased, resulting from the enhanced surface tension between liquid and crystal. Thus, five-fold symmetry favors glass formation and enhances glass-forming ability. This is consistent with the observations in many metallic glass-forming liquids[42] and the current findings. Based on their work,[66] the ease of metallic glass formation under high pressures may result from much severer suppression of crystallization due to the enhanced five-fold symmetry. To further verify the suitability of W in characterizing supercooled dynamics,[42] we show the excellent fittings to Eq. (8) in Fig. 8(c). More significantly, the structural fragility δ in the inset of Fig. 8(c) decreases monotonically with increasing pressure. It means that the sensitivity of τ_α to the structural variation becomes weaker and structure changes more rapidly at higher pressure. These monotonic variations in the kinetic fragility and structural fragility suggest some hidden connection between the static structure and average dynamics.

D. Dynamic heterogeneities

Dynamic heterogeneity is a remarkable feature of glassy dynamics and it has been considered to be the origin of many complex phenomena and properties.[34,67] As can be seen in Fig. 5, the average atomic displacement or MSD is quite smooth; however, when looking at the single particle resolution, the atomic motion is highly intermittent.[67] Upon approaching the glass transition, the atomic mobility of a region is faster or slower by orders of magnitude than the neighboring areas, indicating the collective nature of dynamics.[35] This heterogeneous dynamics has been verified in many experimental and simulation works.[32,34,38,68,69] In fact, the non-exponential feature of the long-time decay of $F_s(q,t)$ depicted in Fig. 6 at low temperatures already implies such cooperative motion in supercooled liquids.

The non-Gaussian parameter $\alpha_2(t)$ characterizes the degree to which particles' displacements deviate from the standard Gaussian distribution. It is frequently utilized to characterize the heterogeneous dynamics of a system at a time interval of t. For a three-dimensional system, it is defined as[70]

$$\alpha_2(t) = \frac{3\left\langle \Delta r^4(t) \right\rangle}{5\left\langle \Delta r^2(t) \right\rangle^2} - 1. \tag{9}$$

In this ternary metallic glass-forming liquid under different pressures, the peak position of $\alpha_2(t)$ is slightly greater than τ_α for high temperatures, but it increases slower during cooling than τ_α and it is much less than τ_α at low temperatures, which is consistent with the previous work.[71] Figure 9(a) shows the typical isothermal variation of $\alpha_2(t)$ under different pressures. It is evident that at a certain temperature, e.g., 1200 K, the peak value $\alpha_{2,max}(T,P)$ and the corresponding time scale increase remarkably. This indicates more heterogeneous dynamics during compressing, similar to the situation upon isobaric cooling.[70] To show the temperature

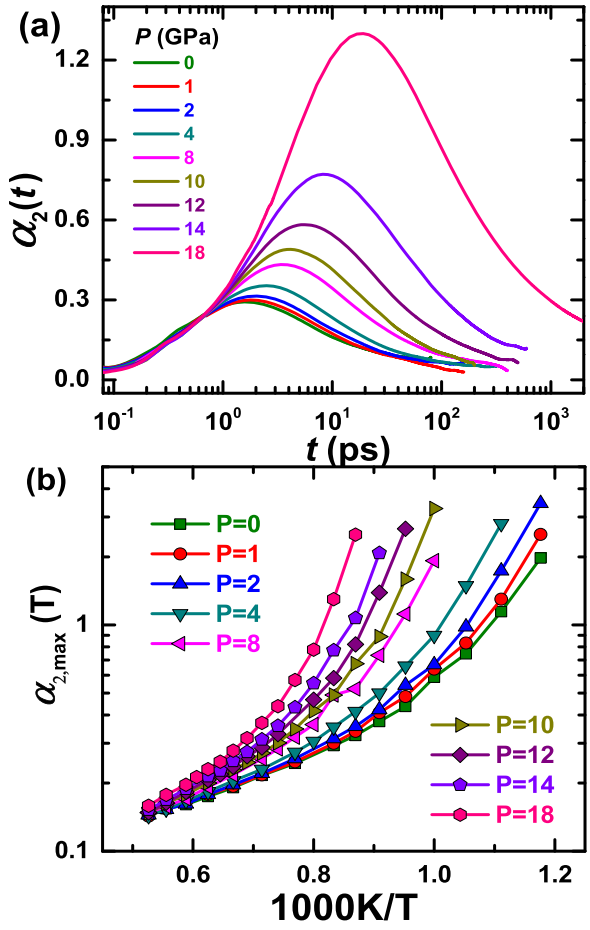

FIG. 9. (a) Non-Gaussian parameter versus time at $T = 1200$ K with pressure spanning from 0 to 18.0 GPa. With increasing pressure, the dynamics becomes more heterogeneous in the metallic liquid. (b) Semi-log plot of the maximums of non-Gaussian parameter at different pressures during cooling. The dynamic heterogeneity is more pronounced at high pressures.

dependence of dynamic heterogeneity under different pressures more clearly, the peak values $\alpha_{2,max}(T,P)$ are depicted in Fig. 9(b). On the ascending of pressure, dynamic heterogeneity becomes more pronounced and increases more rapidly during cooling.

Previous results suggest a correlation between dynamic heterogeneity and fragility.[53,72,73] It is thought that dynamic heterogeneity is comparatively suppressed in strong liquids than fragile ones.[53,72,73] In our current study, the metallic liquid becomes more fragile when pressure is increased (Fig. 8(a)). Meanwhile, the dynamics turns out to be more heterogeneous with the application of high pressures (Fig. 9(b)). Thus, the finding here is coincident with the previous belief that fragile liquids are more heterogeneous.[72,73] Furthermore, as shown in Fig. 4, the enhancement of the locally preferred structure with higher five-fold symmetry with increasing pressure may indicate a more complicated free energy profile for the system, and thus, a more intricate potential energy landscape with numerous well-separated "megabasins." As a consequence, the more fragile liquid under high pressures is more dynamically heterogeneous.[53]

Another popular way to quantify dynamic heterogeneity is estimating the dynamic correlation length.[33,37] In the Adam-Gibbs theory,[35] the concept "cooperatively rearranging region" suggesting dynamic heterogeneity was invoked, but its size and growth were not included. To quantify the length scale, measuring fluctuations of the particles' dynamics is crucial and thus high order correlation functions are required. Previously, the four-point density correlation function was developed to study the dynamic fluctuations in model glass-forming liquids. However, reports on real liquids like metallic system are rare. The four-point, time-dependent, dynamic structure factor $S_4(q,t)$ is defined as

$$S_4(q,t) = \frac{1}{N}\left[\langle W(\mathbf{q},t)\, W(-\mathbf{q},t)\rangle - \langle W(\mathbf{q},t)\rangle \langle W(-\mathbf{q},t)\rangle\right], \tag{10}$$

where $W(\mathbf{q},t) = \sum_{i=1}^{N} \exp\left[i\mathbf{q}\cdot\mathbf{r}_i(0)\right] \omega\left(|\mathbf{r}_i(t) - \mathbf{r}_i(0)|\right)$. To calculate $S_4(q,t)$, the atomic mobility should be characterized at first and thus the overlap function $Q(t) = \sum_{i=1}^{N} \omega\left(|\mathbf{r}_i(t) - \mathbf{r}_i(0)|\right)$ is introduced. The weight function $\omega(r) = 1$ if $r \le 1.0$ Å($\sim 0.3 d_{Zr}$; d_{Zr} is the atomic diameter of Zr), and =0 otherwise.[37,74] Thus, $\langle Q(t)\rangle/N$ represents the fraction of atoms whose displacement is smaller than 1.0 Å over time interval t, so ***slow*** atoms are picked out in this way. The exemplified curves of $\langle Q(t)\rangle/N$ are shown in Fig. 10. $\langle Q(t)\rangle/N$ carries similar information to $F_s(q,t)$. The decay of $\langle Q(t)\rangle/N$ is not exponential in a normal liquid. There is also an alternative method to define τ_α by $\langle Q(\tau_\alpha)\rangle/N = 1/e$, which is popular in model glass-forming liquids. Then the so-called four point dynamic susceptibility $\chi_4(t)$ is defined as $\chi_4(t) = \frac{1}{N}(\langle Q(t)^2\rangle - \langle Q(t)\rangle^2)$. $\chi_4(t)$ reflects the volume of correlated motion. According to the spatial correlation of slow atoms, the dynamic susceptibility and dynamic structure factor of slow domains are calculated and denoted as $\chi_{4,\mathrm{slow}}(t)$ and $S_{4,\mathrm{slow}}(q,t)$, respectively.

However, from the viewpoint of dynamic heterogeneity, it is natural to consider that there are also fast atoms. Previous studies mainly focused on slow atoms defined above and less attention has been paid to fast ones. In this study, similar to the slow atoms, an overlap function $q(t) = \sum_{i=1}^{N} \omega\left(|\mathbf{r}_i(t) - \mathbf{r}_i(0)|\right)$ is also defined. Nevertheless, the weight function $\omega(r) = 1$ if $r \ge 1.60$ Å ($\sim 0.5 d_{Zr}$), and =0 otherwise. Here $\langle q(t)\rangle/N$ represents the fraction of atoms whose displacement is larger than 1.60 Å over the time interval t; thus, the *fast* atoms could be identified. At a longer time, more and more atoms escape from the cage formed by their neighbors, so the trend of $\langle q(t)\rangle/N$ is opposite to that of $\langle Q(t)\rangle/N$ (Fig. 10). Similarly, the dynamic susceptibility and dynamic structure factor of fast atoms are calculated and denoted as $\chi_{4,\mathrm{fast}}(t)$ and $S_{4,\mathrm{fast}}(q,t)$, respectively. Regarding $\chi_4(t)$, it would increase to a peak first and then decays to 0 at a very long time, no matter for slow or fast atoms. These are well observed in Figs. 11(a) and 11(b), in which $\chi_{4,\mathrm{slow}}(t)$ and $\chi_{4,\mathrm{fast}}(t)$ are shown in the isobaric cooling (P = 4.0 GPa) and isothermal compressing (T = 1200 K) processes. During cooling (Fig. 11(a)) or compressing (Fig. 11(b)) in the accessed temperature and pressure ranges, the peak value of $\chi_4(t)$ and the corresponding time scale of slow and fast domains increase remarkably, indicating increasingly heterogeneous state of the liquid. We then calculated the four-point structure factors $S_4(q,\tau_p)$ of the slow and fast atoms at the peak time scales τ_p of $\chi_{4,\mathrm{slow}}(t)$ and $\chi_{4,\mathrm{fast}}(t)$, respectively. Note from Fig. 11 that the peak time scales of the slow atoms are much smaller than those of the fast atoms. An example of $S_{4,\mathrm{slow}}(q,\tau_p)$ is shown in Fig. 12(a), from which the dynamic correlation length $\xi_{4,\mathrm{slow}}$ was extracted by fitting the Ornstein-Zernike function $S_{4,\mathrm{slow}}(q,\tau_p) = \frac{S_{4,\mathrm{slow}}(0)}{1+(q\xi_{4,\mathrm{slow}})^2}$ to $S_{4,\mathrm{slow}}(q,\tau_p)$ for $q \le 1.0$ Å^{-1}. The trends of $S_{4,\mathrm{fast}}(q,\tau_p)$ and the processes to determine $\xi_{4,\mathrm{fast}}$ are similar to those of the slow atoms (not shown here). The smallest accessible data of $S_4(q,\tau_p)$ are related to the lowest wave number restricted by the sample size. It has been shown that to estimate ξ_4 accurately, one either needs a very large system,[75] or one needs to calculate the ensemble independent dynamic susceptibility for the fits and still have a moderately large system.[76] Therefore, due to the limited system size, the correlation lengths obtained for the larger τ_α may be systematically small. However, our primary purpose of this study is to systematically study the effects

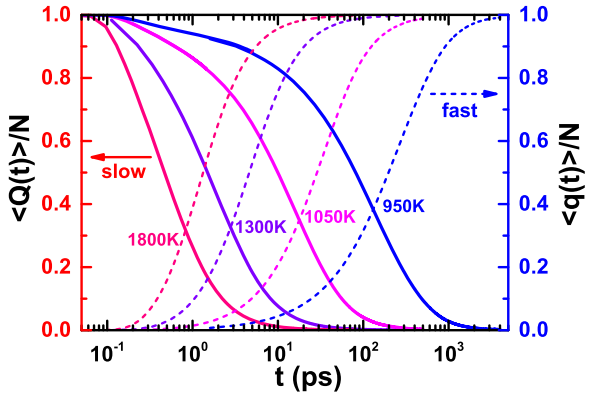

FIG. 10. Overlap functions of the slow (solid, left) and fast (dashed, right) atoms at P = 4.0 GPa. The overlap functions of the slow atoms give similar information to the self-intermediate scattering function in Fig. 6(a). With decreasing temperature, the decay of $\langle Q(t)\rangle/N$ and the increase of $\langle q(t)\rangle/N$ become slower and non-exponential.

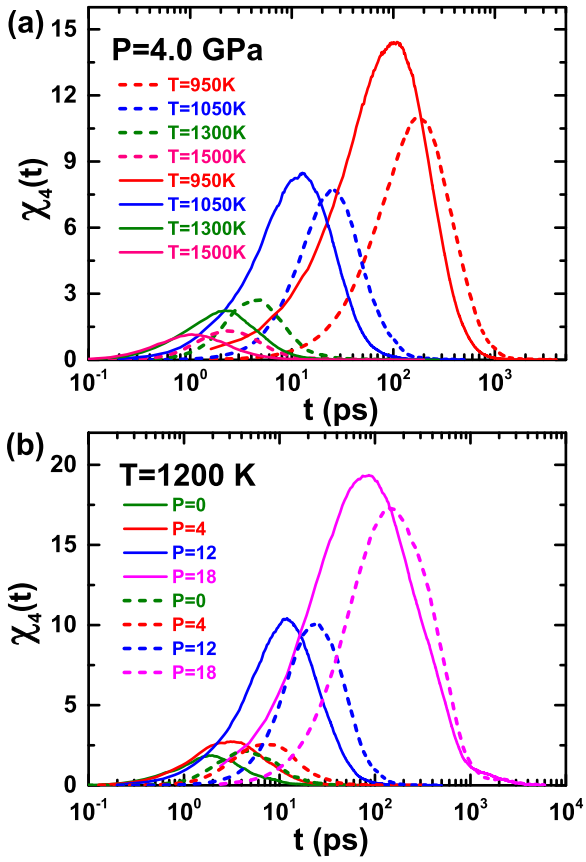

FIG. 11. Dynamic susceptibilities of the slow and fast atoms during isobaric cooling (a) and isothermal compressing (b). Solid lines are for the slow atoms while dashed lines are for the fast ones. In all cases, the susceptibility increases to a peak at a certain time scale and then decreases to zero. The peak time scale of the fast atoms is much larger than that of the slow atoms. The increasing peak value and time scale also indicate a more heterogeneous state.

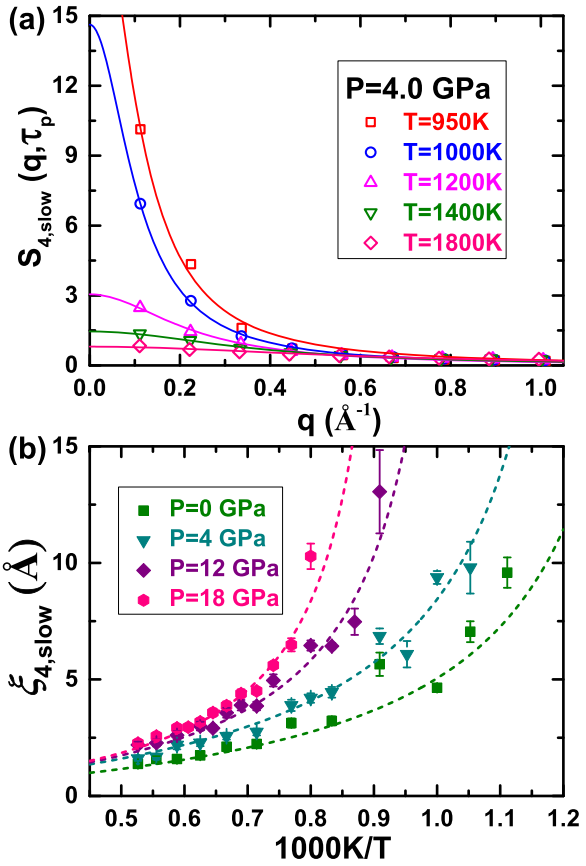

FIG. 12. (a) The four point dynamic structure factors of the slow atoms during cooling at $P = 4.0$ GPa. The solid lines are fittings to the Ornstein-Zernike function to extract the dynamic correlation length; (b) the growing dynamic correlation lengths of the slow atoms during cooling. The dashed lines are fittings to $\xi_4 = BT_0/(T - T_0)$, with T_0 fixed at the value determined from the VFT fittings to the structural relaxation time.

of pressure on the structure and dynamics of the metallic liquids and compare these behaviors under different pressures. As such, the accuracy of the correlation lengths does not qualitatively change our main conclusions. Nevertheless, the accurate determination of the four point correlation length with a larger system is still important, which will be addressed in our future work because huge computational efforts are demanded. The apparent increase of $\xi_{4,\mathrm{slow}}$ during cooling is illustrated in Fig. 12(b). $\xi_{4,\mathrm{slow}}$ increases more rapidly when the pressure is elevated, indicating more heterogeneous state under high pressures, consistent with the previous observations (Figs. 9 and 11). Although there are many relations to describe the growth of dynamic correlation length during cooling or compressing,[33,37] here we found the relation $\xi_4 = BT_0/(T - T_0)$ well captures the growing tendency under different pressures. In this relation, B is a fitting parameter and T_0 is the dynamic ideal glass transition temperature determined from the VFT fittings to the structural relaxation time. This description also indicates some relation between the time scale and length scale.

Instead of showing the growth of $\xi_{4,\mathrm{fast}}$ during cooling directly, we prefer to compare the length scales of the defined fast and slow atoms, i.e., $\xi_{4,\mathrm{fast}}$ and $\xi_{4,\mathrm{slow}}$. Although the extracted dynamic length scales are related to the chosen cutoffs in the weight functions, it has been argued that the cutoff turns out to be qualitatively unimportant. For convenience, the influence stemming from the cutoff could be found in Ref. 77. As shown in Fig. 13, the correlation lengths under different pressures collapse onto a single curve, demonstrating a universal relationship between $\xi_{4,\mathrm{fast}}$ and $\xi_{4,\mathrm{slow}}$. Furthermore, the calculated dynamic correlation lengths of the fast atoms $\xi_{4,\mathrm{fast}}$

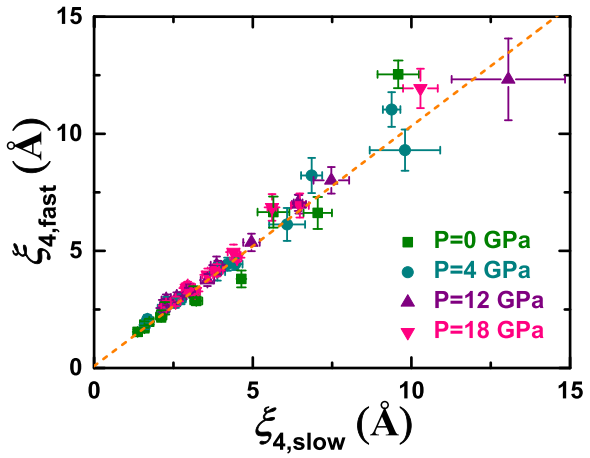

FIG. 13. The dynamic correlation lengths of the fast atoms versus those of the slow atoms. The dashed line is a linear fit. These length scales are comparable with some fluctuations at the larger values.

are nearly equal to the magnitudes of the conventionally considered slow atoms $\xi_{4,\mathrm{slow}}$ under all pressures. This directly evidences the heterogeneous dynamics in the supercooled liquids, in which fast and slow regions coexist. The dynamics is more localized and the spatial correlation lengths grow similarly with decreasing temperature. At high temperatures, the liquid is homogeneous or nearly, it is hard to distinguish slow and fast atoms. So the length scales of these two parts should be small and similar. When temperature is decreased, dynamics becomes heterogeneous and localized, with increasingly localized and cooperative slow and fast regions. Therefore, in this temperature regime, the length scales of both slow and fast atoms would increase, as observed in Fig. 13. Moreover, in the deeply supercooled state under the mode-coupling temperature, the atomic mobility is much lower. Thus we speculate that the length scale of slow atoms would increase while an opposite trend may be observed for the length scale of fast atoms.[78,79] In this study, the results in Fig. 13 are reasonable since the temperature range we considered is not below the mode-coupling temperature. In fact, liquids under this critical temperature are very difficult to equilibrate in computer simulations. Maybe the fast regions shall also be taken into consideration when dynamic heterogeneities are studied in the future.

Finally, we examine the scaling relations between ξ_4 and τ_α in this metallic glass-forming liquid under different pressures, which has not been reported before in any metallic liquids. Finding the relationship between time scale and length scale or clarifying which length scale controls the dramatic growth of time scale is one of the central issues in understanding the glass transition. Many different scaling laws have been proposed from different theories, such as kinetically constrained model, mode-coupling theory, Adam-Gibbs theory and RFOT theory.[33,35–37,80] Here, we simply consider two scaling relations: one is the power law $\xi \sim {\tau_\alpha}^{1/z}$ and the other is an exponential form $\xi^\theta \sim \ln(\tau_\alpha)$. As illustrated in Fig. 14, when the length scales ξ_4 for both slow and fast atoms are plotted as a function of τ_α, all data from different pressures collapse on a master curve, although with some fluctuations at low temperatures. This demonstrates the intrinsic characteristics of length scale and time scale in metallic glass-forming liquids. Moreover, the mode-coupling-like power-law relation fails to describe the data over the whole range with a single exponent $1/z$.[76,81] A much larger exponent or more rapid growth is needed to capture the high temperature results. The value $1/z$ in Fig. 14 is fitted to be about 0.28. However, the relation $\xi^\theta \sim \ln(\tau_\alpha)$ with $\theta \cong 1$ holds well for all of the data (Fig. 14). Notably, Flenner *et al.* also found the same universal relationship in several fragile model glass-forming liquids with different interatomic interactions, but only for slow atoms.[82] Nevertheless, here we take both slow and fast atoms into consideration. It is also necessary to mention that the metallic liquids studied here are also fragile, especially under high pressures. Furthermore, Staley *et al.* observed the breakdown of such a relationship in network-forming, strong glass formers.[83] Thus, the coincidence of the current results with previous works on hard spheres, binary mixture of soft particles, and model glass-forming liquids indicates that this spatiotemporal correlation may be universal for fragile glass formers.[76,82,84,85] The increase of dynamic correlation length with relaxation time is much slower than the predictions of mode-coupling theory. More importantly, the exponential relation is conformable with the spirit of Adam-Gibbs and RFOT theories, although the exponent θ of ξ_4 is smaller than the theoretical values. This disagreement may result from the difference between the static point-to-set correlation length in the RFOT theory and the dynamic correlation length from the four point dynamic structure factor studied here. However, through numerical studies, Cammarota *et al.* found that the exponent of the size of the correlated regions or the correlation length is nearly equal to unity in a model glass former.[84] Furthermore, a similar exponent around unity was also observed in the monodisperse hard-sphere metastable liquids with some pinning particles in a periodic array manner.[85] Hence, future work is required to clarify the connection between the static correlation length and the dynamic correlation length, as well as the scaling relation between length scale and time scale.

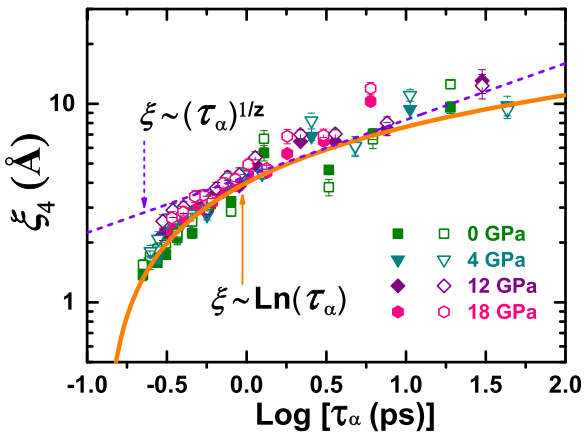

FIG. 14. The scaling relations between the correlation lengths and relaxation times. The filled symbols are for the slow atoms while the open symbols are for the fast atoms. The dashed and solid lines are $\xi \sim {\tau_\alpha}^{1/z}$ and $\xi \sim \ln(\tau_\alpha)$ fittings to the correlation lengths of the slow atoms. Obviously, the form $\xi \sim \ln(\tau_\alpha)$ fits well over the whole range of the data and similar behavior could be found for the fast atoms.

IV. CONCLUSION

We systematically studied the structure and dynamics of a ternary $Zr_{50}Cu_{44}Al_6$ metallic glass-forming liquid under positive external hydrostatic pressures by molecular dynamics simulations. Both isobaric cooling and isothermal compressing make glass-forming liquids become increasingly viscous and form glasses when the relaxation time is too long to equilibrate. In spite of the similar densification characteristics of the overall static structure during cooling and compressing, there are still significant differences in the effects of temperature and pressure on the local coordination structures at the short-range. The improved local ordering at high pressure and low temperature was also identified from the decreased pair structural entropy and the increased five-fold local symmetry.

Meanwhile, the slowdown of the average dynamics and the rise of the glass transition temperature with increasing

pressure demonstrate that pressure can significantly affect the dynamics of metallic glass-forming liquids. The effects of pressure and temperature on the fragility are different, which may correlate with the evolution of the locally preferred structures. Furthermore, we found that the structural parameter, the average five-fold local symmetry, also captures the structural evolution under high pressures and is associated with the dramatic slowdown of glassy dynamics. The derived structural fragility varies monotonously when pressure is increased. These findings suggest a structural basis for the kinetic fragility.

Finally, the dynamic heterogeneities of the metallic liquids under different pressures were characterized by the non-Gaussian parameter and the dynamic correlation length. The latter was examined for both the slow atoms and the fast ones by analyzing the four-point dynamic structure factor. When comparing the degree of dynamic heterogeneities at different state points, larger pressure is found to promote more heterogeneous dynamics from these two measurements. The coexistence and growth of the correlation lengths of the fast and slow regions also directly reveal the heterogeneous feature of supercooled liquids. As for the scaling relation between time scale and length scale, we found that the exponential form consistent with the spirit of the Adam-Gibbs and RFOT theories describes all the data in the whole range well, rather than the mode-coupling-like power-law relation. Although future simulations with larger systems are needed to estimate more accurate values of the dynamic correlation lengths for low temperatures, the sample size limitation here would not alter our conclusions qualitatively. Moreover, the coincidence of this result with previous works on other glass-forming systems indicates that this spatiotemporal correlation is likely universal for both slow and fast atoms among fragile glass formers. The correlation and difference between the dynamic correlation length and the static correlation length, and the scaling relations between time scale and these length scales deserve future investigation.

Since pressure plays an important role in the glass transition, as temperature does, theories dealing with the issues of glass transition and the related problems shall take pressure effects into consideration. Our findings provide some fundamentals for further investigating the structure and dynamical behaviors of metallic glass-formers and may shed light on understanding liquids and glasses.

ACKNOWLEDGMENTS

We acknowledge helpful discussions with Y. W. Li, W. S. Xu, M. X. Pan, D. W. Ding, and B. B. Wang. This work is supported by National Natural Science Foundation of China (NSFC) Grant Nos. 51571209, 51461165101, and 51571011, the Ministry of Science and Technology of the People's Republic of China 973 Program (No. 2015CB856800), and the Key Research Program of Frontier Sciences, CAS (QYZDY-SSW-JSC017). Y.Y. is supported by Research Grant Council (RGC), the Hong Kong Government, through the General Research Fund (GRF) with Grant No. CityU11207215, and through the RGC-NSFC joint fund with Grant No. N_CityU116/14. We also acknowledge the computational support from the Beijing Computational Science Research Center (CSRC).

[1] W. L. Johnson, MRS Bull. **24**, 42 (1999).
[2] W. H. Wang, C. Dong, and C. H. Shek, Mater. Sci. Eng., R **44**, 45 (2004).
[3] J. Schroers, Phys. Today **66**, 32 (2013).
[4] A. L. Greer, Science **267**, 1947 (1995).
[5] A. Inoue, B. Shen, H. Koshiba, H. Kato, and A. R. Yavari, Nat. Mater. **2**, 661 (2003).
[6] M. D. Demetriou, M. E. Launey, G. Garrett, J. P. Schramm, D. C. Hofmann, W. L. Johnson, and R. O. Ritchie, Nat. Mater. **10**, 123 (2011).
[7] J. Schroers, Adv. Mater. **22**, 1566 (2010).
[8] G. Kumar, H. X. Tang, and J. Schroers, Nature **457**, 868 (2009).
[9] H.-J. Yu, J.-Q. Wang, X.-T. Shi, D. V. Louzguine-Luzgin, H.-K. Wu, and J. H. Perepezko, Adv. Funct. Mater. **23**, 4793 (2013).
[10] J. Schroers, G. Kumar, T. Hodges, S. Chan, and T. Kyriakides, JOM **61**, 21 (2009).
[11] Y. C. Hu, Y. Z. Wang, R. Su, C. R. Cao, F. Li, C. W. Sun, Y. Yang, P. F. Guan, D. W. Ding, Z. L. Wang, and W. H. Wang, Adv. Mater. **28**, 10293 (2016).
[12] M. Ediger, C. Angell, and S. R. Nagel, J. Phys. Chem. **100**, 13200 (1996).
[13] C. P. Royall and S. R. Williams, Phys. Rep. **560**, 1 (2015).
[14] P. J. Steinhardt, D. R. Nelson, and M. Ronchetti, Phys. Rev. B **28**, 784 (1983).
[15] H. Tanaka, Eur. Phys. J. E **35**(10), 113 (2012).
[16] V. A. Borodin, Philos. Mag. A **79**, 1887 (1999).
[17] F. W. Starr, S. Harrington, F. Sciortino, and H. E. Stanley, Phys. Rev. Lett. **82**, 3629 (1999).
[18] C. M. Roland, S. Hensel-Bielowka, M. Paluch, and R. Casalini, Rep. Prog. Phys. **68**, 1405 (2005).
[19] K. Golden, B. Jerzy, and S. Jan, Nanotechnology **24**, 105301 (2013).
[20] Q. Luo, G. Garbarino, B. Sun, D. Fan, Y. Zhang, Z. Wang, Y. Sun, J. Jiao, X. Li, P. Li, N. Mattern, J. Eckert, and J. Shen, Nat. Commun. **6**, 5703 (2015).
[21] D. Wakabayashi, N. Funamori, and T. Sato, Phys. Rev. B **91**, 014106 (2015).
[22] V. Trappe, V. Prasad, L. Cipelletti, P. N. Segre, and D. A. Weitz, Nature **411**, 772 (2001).
[23] J. Q. Wang and H. Y. Bai, Scr. Mater. **61**, 453 (2009).
[24] M. Wu, J. S. Tse, S. Y. Wang, C. Z. Wang, and J. Z. Jiang, Nat. Commun. **6**, 6493 (2015).
[25] J. Caris and J. J. Lewandowski, Acta Mater. **58**, 1026 (2010).
[26] L. M. Martinez and C. A. Angell, Nature **410**, 663 (2001).
[27] R. Casalini and C. M. Roland, Phys. Rev. B **71**, 014210 (2005).
[28] A. A. Pronin, M. V. Kondrin, A. G. Lyapin, V. V. Brazhkin, A. A. Volkov, P. Lunkenheimer, and A. Loidl, Phys. Rev. E **81**, 041503 (2010).
[29] S. Pawlus, M. Paluch, J. Ziolo, and C. M. Roland, J. Phys.: Condens. Matter **21**, 332101 (2009).
[30] M. Paluch, R. Casalini, S. Hensel-Bielowka, and C. M. Roland, J. Chem. Phys. **116**, 9839 (2002).
[31] H. Shintani and H. Tanaka, Nat. Mater. **7**, 870 (2008).
[32] L. Berthier, G. Biroli, J.-P. Bouchaud, L. Cipelletti, D. E. Masri, D. L'Hôte, F. Ladieu, and M. Pierno, Science **310**, 1797 (2005).
[33] S. Karmakar, C. Dasgupta, and S. Sastry, Annu. Rev. Condens. Matter Phys. **5**, 255 (2014).
[34] M. D. Ediger, Annu. Rev. Phys. Chem. **51**, 99 (2000).
[35] G. Adam and J. H. Gibbs, J. Chem. Phys. **43**, 139 (1965).
[36] T. R. Kirkpatrick and D. Thirumalai, Rev. Mod. Phys. **87**, 183 (2015).
[37] N. Lačević, F. W. Starr, T. B. Schrøder, and S. C. Glotzer, J. Chem. Phys. **119**, 7372 (2003).
[38] L. Berthier and G. Biroli, Rev. Mod. Phys. **83**, 587 (2011).
[39] A. Cavagna, Phys. Rep. **476**, 51 (2009).
[40] S. Plimpton, J. Comput. Phys. **117**, 1 (1995).
[41] Y. Cheng, E. Ma, and H. W. Sheng, Phys. Rev. Lett. **102**, 245501 (2009).
[42] Y. C. Hu, F. X. Li, M. Z. Li, H. Y. Bai, and W. H. Wang, Nat. Commun. **6**, 8310 (2015).
[43] C. Patrick Royall, S. R. Williams, T. Ohtsuka, and H. Tanaka, Nat. Mater. **7**, 556 (2008).
[44] H. Peng, M. Li, and W. Wang, Phys. Rev. Lett. **106**, 135503 (2011).
[45] Y. Q. Cheng and E. Ma, Prog. Mater. Sci. **56**, 379 (2011).
[46] H. Sheng, W. Luo, F. Alamgir, J. Bai, and E. Ma, Nature **439**, 419 (2006).
[47] D. B. Miracle, W. S. Sanders, and O. N. Senkov, Philos. Mag. **83**, 2409 (2003).
[48] J. Mittal, J. R. Errington, and T. M. Truskett, J. Phys. Chem. B **110**, 18147 (2006).

[49]A. Banerjee, S. Sengupta, S. Sastry, and S. M. Bhattacharyya, Phys. Rev. Lett. **113**, 225701 (2014).
[50]Y. C. Hu, F. X. Li, M. Z. Li, H. Y. Bai, and W. H. Wang, J. Appl. Phys. **119**, 205108 (2016).
[51]S. P. Das, Rev. Mod. Phys. **76**, 785 (2004).
[52]W. Kob and H. C. Andersen, Phys. Rev. E **52**, 4134 (1995).
[53]P. G. Debenedetti and F. H. Stillinger, Nature **410**, 259 (2001).
[54]Y. Q. Cheng, H. W. Sheng, and E. Ma, Phys. Rev. B **78**, 014207 (2008).
[55]K. Samwer, R. Busch, and W. L. Johnson, Phys. Rev. Lett. **82**, 580 (1999).
[56]K. Adrjanowicz, Z. Wojnarowska, M. Paluch, and J. Pionteck, J. Phys. Chem. B **115**, 4559 (2011).
[57]S. P. Andersson and O. Andersson, Macromolecules **31**, 2999 (1998).
[58]C. A. Angell, Science **267**, 1924 (1995).
[59]R. Böhmer, K. L. Ngai, C. A. Angell, and D. J. Plazek, J. Chem. Phys. **99**, 4201 (1993).
[60]D. Coslovich and G. Pastore, J. Chem. Phys. **127**, 124504 (2007).
[61]N. A. Mauro, M. Blodgett, M. L. Johnson, A. J. Vogt, and K. F. Kelton, Nat. Commun. **5**, 4616 (2014).
[62]S. Wei, M. Stolpe, O. Gross, Z. Evenson, I. Gallino, W. Hembree, J. Bednarcik, J. J. Kruzic, and R. Busch, Appl. Phys. Lett. **106**, 181901 (2015).
[63]S. Sastry, Nature **409**, 164 (2001).
[64]M. Paluch, J. Gapinski, A. Patkowski, and E. W. Fischer, J. Chem. Phys. **114**, 8048 (2001).
[65]H. Tanaka, J. Non-Cryst. Solids **351**, 678 (2005).
[66]J. Taffs and C. Patrick Royall, Nat. Commun. **7**, 13225 (2016).
[67]L. Berthier, G. Biroli, J.-P. Bouchaud, L. Cipelletti, and W. van Saarloos, *Dynamical Heterogeneities in Glasses, Colloids, and Granular Media* (Oxford University Press, 2011).
[68]M. M. Hurley and P. Harrowell, Phys. Rev. E **52**, 1694 (1995).
[69]A. Widmer-Cooper, P. Harrowell, and H. Fynewever, Phys. Rev. Lett. **93**, 135701 (2004).
[70]W. Kob, C. Donati, S. J. Plimpton, P. H. Poole, and S. C. Glotzer, Phys. Rev. Lett. **79**, 2827 (1997).
[71]E. Flenner and G. Szamel, Phys. Rev. E **72**, 031508 (2005).
[72]H.-B. Yu, R. Richert, R. Maasz, and K. Samwer, Nat. Commun. **6**, 7179 (2015).
[73]P. Bordat, F. Affouard, M. Descamps, and K. Ngai, Phys. Rev. Lett. **93**, 105502 (2004).
[74]Y.-C. Hu, B.-S. Shang, P.-F. Guan, Y. Yang, H.-Y. Bai, and W.-H. Wang, J. Chem. Phys. **145**, 104503 (2016).
[75]S. Karmakar, C. Dasgupta, and S. Sastry, Phys. Rev. Lett. **105**, 015701 (2010).
[76]E. Flenner and G. Szamel, Phys. Rev. Lett. **105**, 217801 (2010).
[77]O. Dauchot, G. Marty, and G. Biroli, Phys. Rev. Lett. **95**, 265701 (2005).
[78]W. Kob, S. Roldan-Vargas, and L. Berthier, Nat. Phys. **8**, 164 (2012).
[79]E. Flenner and G. Szamel, Nat. Phys. **8**, 696 (2012).
[80]A. S. Keys, L. O. Hedges, J. P. Garrahan, S. C. Glotzer, and D. Chandler, Phys. Rev. X **1**, 021013 (2011).
[81]K. Kim, S. Saito, K. Miyazaki, G. Biroli, and D. R. Reichman, J. Phys. Chem. B **117**, 13259 (2013).
[82]E. Flenner, H. Staley, and G. Szamel, Phys. Rev. Lett. **112**, 097801 (2014).
[83]H. Staley, E. Flenner, and G. Szamel, J. Chem. Phys. **143**, 244501 (2015).
[84]C. Cammarota, A. Cavagna, G. Gradenigo, T. S. Grigera, and P. Verrocchio, J. Chem. Phys. **131**, 194901 (2009).
[85]Y. Zhou and S. T. Milner, Soft Matter **12**, 402 (2016).